

A VARIABLE GAIN-LIMITED INVERSE Q FILTERING METHOD TO ENHANCE THE RESOLUTION OF SEISMIC DATA

YU SHI¹, HUAI-LAI ZHOU², CONG NIU³, CHUN-CHENG LIU³ and LING-JUN MENG²

¹ College of Geophysics, Chengdu University of Technology, Chengdu, Sichuan 610059, P.R. China. Sichuan Coalfield Geology Bureau, Chengdu 610072, P.R. China. geo.shiyu@foxmail.com

² State Key Laboratory of Oil and Gas Reservoir Geology and Exploitation, Key Lab of Earth Exploration and Information Techniques of Ministry of Education, College of Geophysics, Chengdu University of Technology, Chengdu, Sichuan 610059, P.R. China. zhouhuailai06@cdut.cn

³ CNOOC Research Institute, Beijing 100027, P.R. China.

(Received May 29, 2018; revised version accepted April 16, 2019)

ABSTRACT

Shi, Y., Zhou, H.L., Niu, C., Liu, C.C. and Meng, L.J., 2019. A variable gain-limited inverse Q filtering method to enhance the resolution of seismic data. *Journal of Seismic Exploration*, 28: 257-276.

Energy absorption, quantified by the quality factor Q , is the main factor of seismic wave attenuation and phase distortion. Inverse Q filtering, which is the inverse process of absorption, can not only effectively compensate the seismic wave attenuation but also correct phase distortion. Stabilized inverse Q filter is a relatively stable inverse Q filtering method. This method effectively overcomes the numerical instability problem while correcting phases distortion and compensating attenuation. However, because of the static nature of the stabilization factor, it may not effectively compensate the attenuation in the deep section or suppress environmental noise when the stabilization factor is less than the optimal. Based on the stabilized inverse Q filter, in this paper, we propose a variable gain-limited inverse Q filtering method to improve the resolution of seismic data. The proposed method contains gain limit and stabilization factor varied with time and Q value, resulting in a more stable and effective gain control. In the applications of both synthetic and field data, we demonstrate that the proposed method can effectively compensate deep energy attenuation and suppress environmental noise, improving the resolution of seismic data without deteriorating signal-to-noise ratio of seismic data. In addition, we calibrate the algorithm proposed in this paper on the enhanced resolution seismic data, showing the value on improving the inversion accuracy.

KEY WORDS: absorption attenuation, inverse Q filtering, gain-control, stabilization factor, signal-noise ratio.

INTRODUCTION

Due to the anelastic nature of the earth media, the seismic wave energy is absorbed and the wavelet is distorted during propagation through the earth, which greatly reduce the resolution of seismic data. Inverse Q filtering is the reverse process of absorption of stratum. It effectively compensates amplitude attenuation, extends frequency band, and corrects phase distortion, improving seismic data resolution so that more accurate thin layer identification and reservoir prediction can be achieved.

Stability control, computation efficiency, and compensation effect summarize the key research problems in inverse Q filtering. Based on Kolske-Futterman model, Hale (1982) put forward an inverse Q filtering method by series expansion approximation to compensate the high frequency component. However, the relatively high computational cost limits this method for large scale application. Hargreaves (1991) proposed an inverse Q filtering method similar to Stolt migration (1978). Using the fast Fourier transform, this method can effectively correct phase distortion. The stabilized inverse Q filter (Wang, 2002) not only effectively overcomes the numerical instability, but also corrects phase distortion caused by dispersion and compensates the amplitude attenuation at the same time. Unfortunately, similar to the gain-limited inverse Q filter (Bickel and Natarajan, 1985), the gain limit (the maximum value of amplitude-compensation function) in the stabilized inverse Q filter is a fixed value only related to stabilization factor, invariant with time and layer Q value. When gain limit is small, the method cannot effectively compensate the attenuation in deeper sections; when gain limit is large, it can effectively compensate the attenuation in deeper sections, but at the expense of effectively suppressing environmental noise, leading to lower signal-to-noise ratio. To resolve this dilemma, Zhang et al. (2015) introduced a self-adaptive approach for inverse Q filtering. Based on seismic data dynamic range, this method effectively suppresses the high frequency noise, but broader application of this method is limited by its implementation complexity.

In addition, Yao et al. (2003) took inverse Q filter to the depth domain. Margrave et al. (2011) Proposed time-frequency domain deconvolution and Zhou et al. (2016) improved this method. Yan et al. (2011) used inverse Q filter on the VSP seismic record, and Liu et al. (2013) proposed a stable inverse Q filtering using the iterative filtering method, reducing the instability of the amplitude compensation in the low and medium frequency components in the inverse Q filtering. Chen et al. (2014) proposed a band-limited and robust inverse Q filtering algorithm to improve the robustness by combining with time-varying band-pass filter. By introducing a frequency-varying band calculation method, Wu et al. (2016) made inverse Q filter more stable.

Inspired by the previous works, in this paper, we propose a variable gain-limited inverse Q filtering method. We design gain-limited and stabilization factors varying with time and layer Q , making the gain control

more stable and effective. Using synthetic test and field application, we demonstrate that the proposed method can not only effectively compensate the energy attenuation in the deep stratum, but also suppress environmental noise, improving seismic resolution without lowering signal-to-noise ratio. In addition, the application in the inversion process also shows that the inversion accuracy can be effectively improved using the enhanced resolution field data processed by our proposed method compared with the original field data.

THEORY AND METHOD

Inverse Q filtering theory

Based on the frequency independent assumption, Futterman (1962) derived seismic wave attenuation and dispersion using 1D wave equation. Seismic wave attenuation described by Kolske-Futterman model is as follows:

$$P(\tau + \Delta\tau, \omega) = P(\tau, \omega) \exp\left[-\left(\frac{\omega}{\omega_h}\right)^{-\gamma} \frac{\omega\Delta\tau}{2Q}\right] \exp\left[-i\left(\frac{\omega}{\omega_h}\right)^{-\gamma} \omega\Delta\tau\right], \quad (1)$$

where $P(\tau, \omega)$ is the seismic wavefield, τ and Q are the time and the quality factors, $\omega = 2\pi f$ is the angular frequency, $\gamma = 1/(\pi Q)$, and $i = \sqrt{-1}$.

An inverse Q filter attempts to compensate the energy loss, correct the wavelet distortion in terms of the shape and timing, and produce a seismic image with high resolution. Normally, we can describe phase correction and amplitude compensation separately:

(1) phase-only inverse Q filtering

$$P(\tau + \Delta\tau, \omega) = P(\tau, \omega) \exp\left[i\left(\frac{\omega}{\omega_h}\right)^{-\gamma} \omega\Delta\tau\right], \quad (2)$$

(2) amplitude-only inverse Q filtering

$$P(\tau + \Delta\tau, \omega) = P(\tau, \omega) \exp\left[\left(\frac{\omega}{\omega_h}\right)^{-\gamma} \frac{\omega\Delta\tau}{2Q}\right], \quad (3)$$

(3) and both

$$P(\tau + \Delta\tau, \omega) = P(\tau, \omega) \exp\left[\left(\frac{\omega}{\omega_h}\right)^{-\gamma} \frac{\omega\Delta\tau}{2Q}\right] \exp\left[i\left(\frac{\omega}{\omega_h}\right)^{-\gamma} \omega\Delta\tau\right]. \quad (4)$$

Stabilized inverse Q filter

Wang (2002) put forward a stable and efficient inverse Q filtering method. This method, by adding a stabilization factor, can compensate amplitude attenuation and correct phase distortion simultaneously without amplifying the ambient noise. This method can be summarized as

$$P(\tau + \Delta\tau, \omega) = P(\tau, \omega)\Lambda(\tau, \omega)\exp\left[i\left(\frac{\omega}{\omega_h}\right)^{-\gamma}\omega\Delta\tau\right], \quad (5)$$

where $\Lambda(\tau, \omega)$ is the amplitude compensation function expressed by

$$\Lambda(\tau, \omega) = \frac{\beta(\tau, \omega) + \sigma^2}{\beta^2(\tau, \omega) + \sigma^2}, \quad (6)$$

$$\beta(\tau, \omega) = \exp\left[-\left(\frac{\omega}{\omega_h}\right)^{-\gamma}\frac{\omega\Delta\tau}{2Q}\right]. \quad (7)$$

In eq. (6), σ^2 is a small real positive constant used to stabilize the solution.

Although the amplitude-compensation coefficient depends on both the Q value and the stabilization factor, its maximum gain only depends on the stabilization factor. Fig. 1 shows the stabilized inverse Q filter gain control function. Because the stabilization factor is a constant, we cannot effectively compensate the attenuation in the deep section if the stabilization factor is too large. When the stabilization factor is small, we can effectively compensate the attenuation in the deep section, but is unable to effectively suppress environmental noise. Moreover, when the stabilization factor approaches to zero, the stabilized inverse Q filter reduces to the conventional inverse Q filter and causes numerical error.

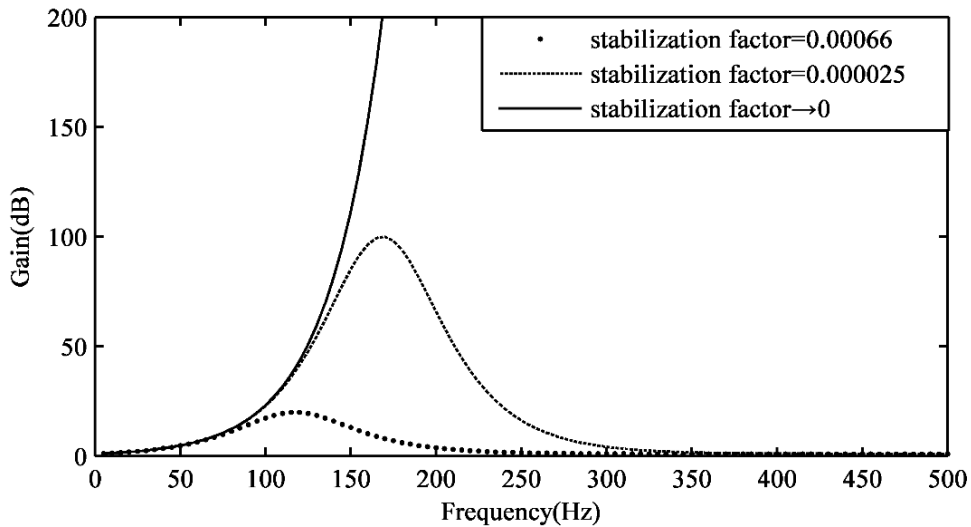


Fig. 1. The stabilized inverse Q filter gain-control function. Stabilization factor is set to 0.00066, 0.000025, and infinitely small.

Variable gain-limited inverse Q filter

Inspired by the stabilized inverse Q filter, in this study, we propose a variable gain-limited inverse Q filtering method. This method sets gain limit and stabilization factor that varies with time and Q . Using a gain control adaptive to amplitude-attenuation, this method can effectively compensate the attenuation in deep section without boosting high frequency noise. We set the gain limit as

$$L = \frac{Q_C(1 + \Delta\tau)}{Q_t}, \quad (8)$$

where L and $\Delta\tau$ are the gain limit and the interval time. The quality factor Q_t is a time-dependent function, Q_C is the basic reference quality factor (if Q_t equal to or greater than Q_C the attenuation can be neglected, in this paper we suppose $Q_C=1000$, that is to say the stratum is ideal without absorption), and Q_t should be less than Q_C because of absorption effects of actual stratum. Note that the gain limit L varies with time and quality factor.

From the stabilized inverse Q filter, we now derive the gain limit (L) and stabilization factor (σ^2). The stabilized inverse Q filter's amplitude-compensation function (Wang, 2002) is defined as

$$\Lambda(\tau, \omega) = \frac{\frac{1}{A(\tau, \omega)} + \sigma^2}{\frac{1}{A^2(\tau, \omega)} + \sigma^2}, \quad (9)$$

in which traditional amplitude-compensation function $A(\tau, \omega)$ is defined as

$$A(\tau, \omega) = \exp\left[\left(\frac{\omega}{\omega_h}\right)^{-\gamma} \frac{\omega\Delta\tau}{2Q}\right]. \quad (10)$$

Eq. (9) can be simplified by

$$\Lambda(\tau, \omega) = \frac{A^2(\tau, \omega) + \alpha A(\tau, \omega)}{A^2(\tau, \omega) + \alpha}, \quad (11)$$

where $\alpha = 1/\sigma^2$ is the reciprocal of stabilization factor. If ω_L is the angular frequency corresponding to the maximum of amplitude-compensation function, the gain limit L can be expressed by

$$L = \Lambda(\tau, \omega_L) = \frac{A^2(\tau, \omega_L) + \alpha A(\tau, \omega_L)}{A^2(\tau, \omega_L) + \alpha}. \quad (12)$$

When the amplitude compensation function is at maximum, the derivative with respect to $A(\tau, \omega)$ is zero. By setting the derivative to zero, we get

$$\alpha = A^2(\tau, \omega_L) - 2A(\tau, \omega_L). \quad (13)$$

Bring eq. (13) into eq. (12), amplitude-compensation function can be expressed as

$$\Lambda(\tau, \omega_L) = 0.5A(\tau, \omega_L). \quad (14)$$

Namely substituting eq. (14) into eq. (12), we can obtain

$$A(\tau, \omega_L) = 2L, \quad (15)$$

and then bring eq. (15) into eq. (13), the reciprocal of stabilization factor can be derived as

$$\alpha = 4L^2 - 4L. \quad (16)$$

Finally, based on the above derivation, we obtain the relation expression between the stabilization factor σ^2 and the gain limit L , expressed as

$$\sigma^2 = \frac{1}{4L^2 - 4L}. \quad (17)$$

By combining eqs. (17) and (8), we can obtain the new relation expression,

$$\sigma^2 = \frac{Q_t^2}{4Q_C^2(1 + \Delta\tau)^2 - 4Q_tQ_C(1 + \Delta\tau)}. \quad (18)$$

Fig. 2 shows the various time gain control function when Q equals to 100. Fig. 2a is the gain control function of stabilized inverse Q filter method with gain limit of 20 dB. Fig. 2b is the gain control function from the proposed method. Note that the gain limit is a constant (Fig. 2a) in stabilized inverse Q filter method, while varying with time (Fig. 2b) in the proposed method. So the compensation method using the variable gain limit approximately accords with the attenuation law when seismic energy spreads through a heterogeneous, anelastic subsurface.

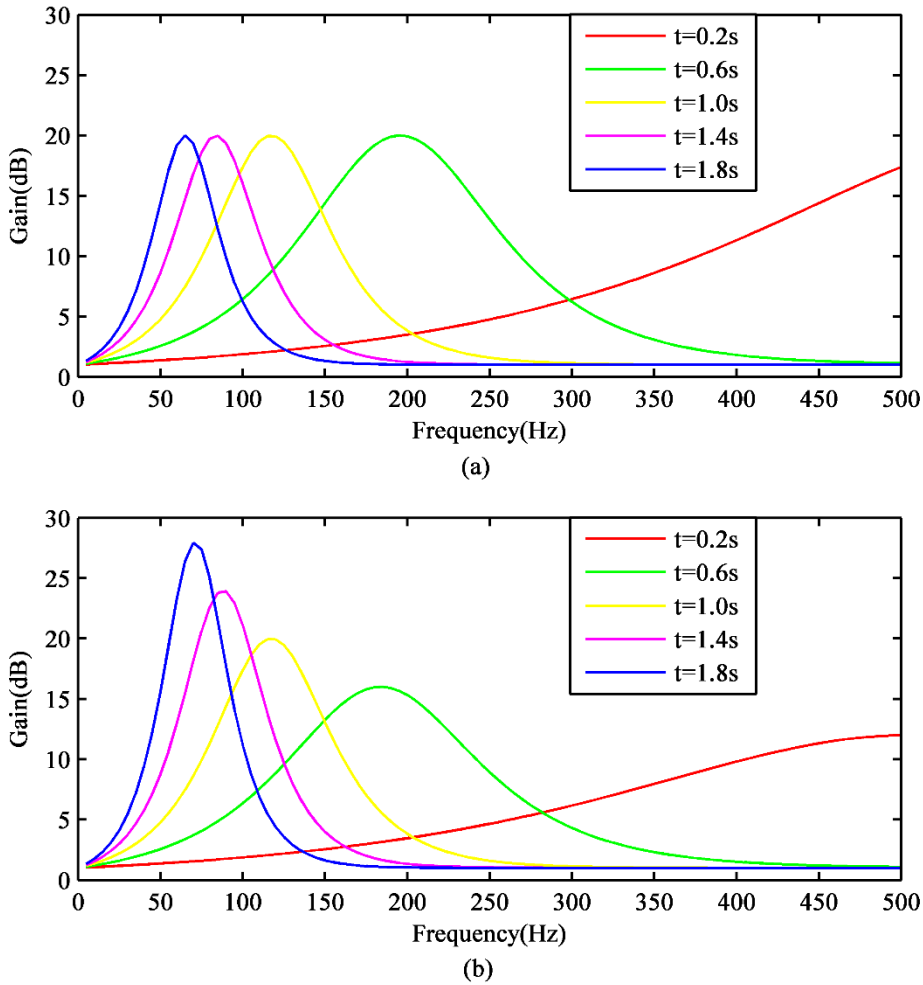


Fig. 2. Different time gain-control function ($Q = 100$). (a) Stabilized inverse Q filter ($L = 20$ dB); (b) Variable gain-limited inverse Q filter.

APPLICATION

We demonstrate the effectiveness and advantage of the variable gain-limited inverse Q filtering method proposed in this paper on synthetic data and field data from Western china and South China Sea.

Synthetic test

In order to verify the effects of the variable gain-limited inverse Q filtering method, we firstly generate a suite of synthetic models with six constant Q values for testing ($Q = 1000, 500, 200, 100, 50$, and 25). Fig. 3a displays six synthetic traces with model Q values. Figs. 3b and 3c display the result from the stabilized inverse Q filtering with gain limit at 20 dB and 60 dB, respectively. The result shows that stabilized inverse Q filtering performs well in the shallow region. When we analyze the wavelet frequency spectrum in the segment within the red dotted box ($Q = 50$,

$t=1.8$ s), we notice that by setting the gain limit to 60 dB, the wavelet frequency band has broadened, with increase in dominant frequency, comparing to the result from 20 dB gain limit. Fig. 3d shows the result from variable gain-limited inverse Q filtering, in which the amplitude of both the shallow and deep regions have achieved good compensation. Fig. 4d is the wavelet frequency spectrum in the red dotted box ($Q = 50$, $t = 1.8$ s) in Fig. 3d. Comparing to Figs. 4b and 4c, the wavelet band from the proposed variable gain-limited inverse Q filtering method is obviously widened with an increase of dominant frequency, therefore the compensation effect is superior to the conventional stabilized inverse Q filtering with gain limit of 20 dB and 60 dB.

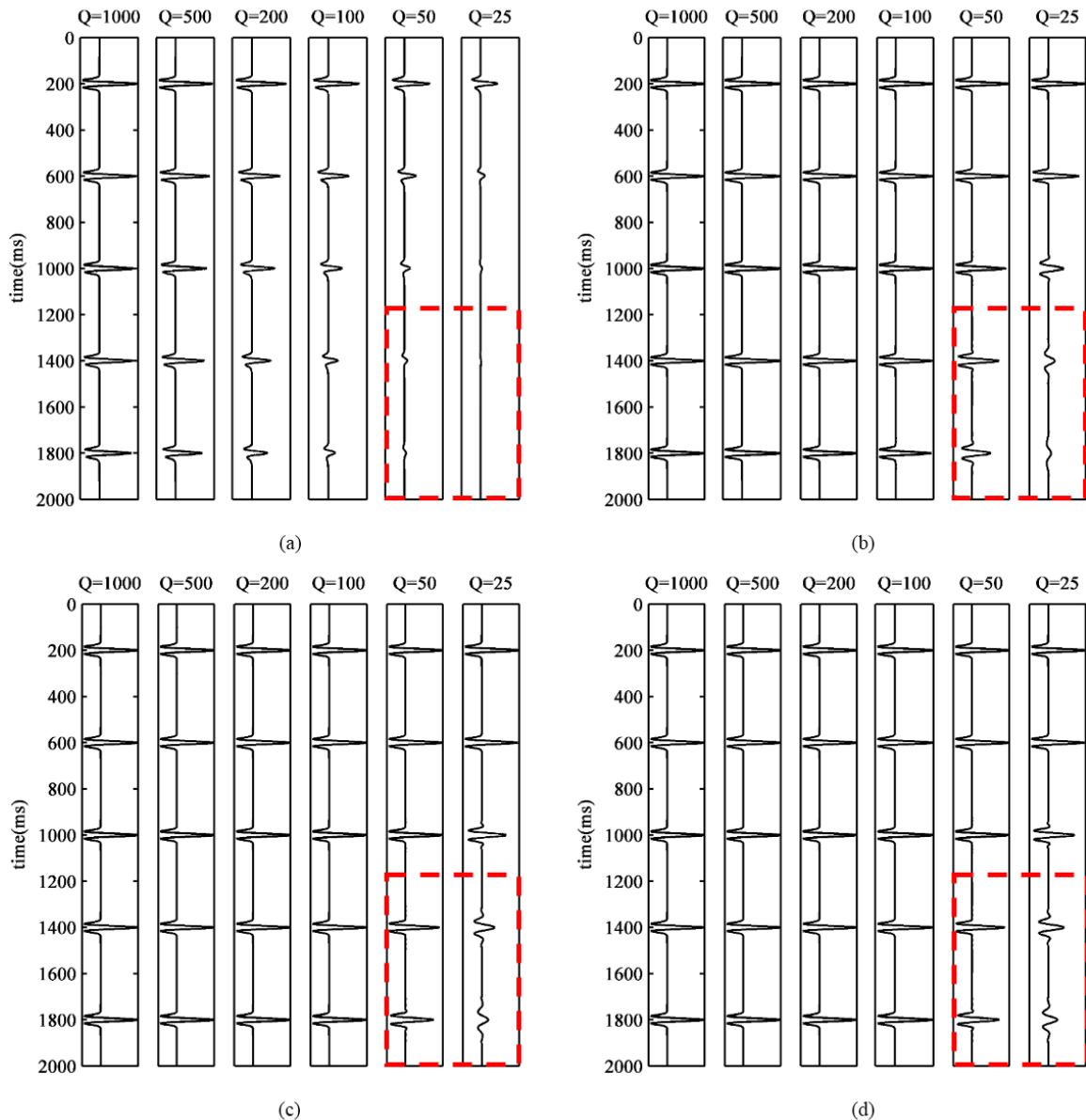


Fig. 3. Noise-free synthetic traces and the results from the two inverse Q filtering algorithms. (a) Synthetic seismic traces with the effect of earth Q filtering with different Q values. (b) The result of the stabilized inverse Q filtering ($L = 20$ dB). (c) The result of the stabilized inverse Q filtering ($L = 60$ dB). (d) The result of the variable gain-limited inverse Q filtering. Note that the attenuation compensation is improved in the variable gain-limited inverse Q filtering result comparing to the stabilized inverse Q filtering.

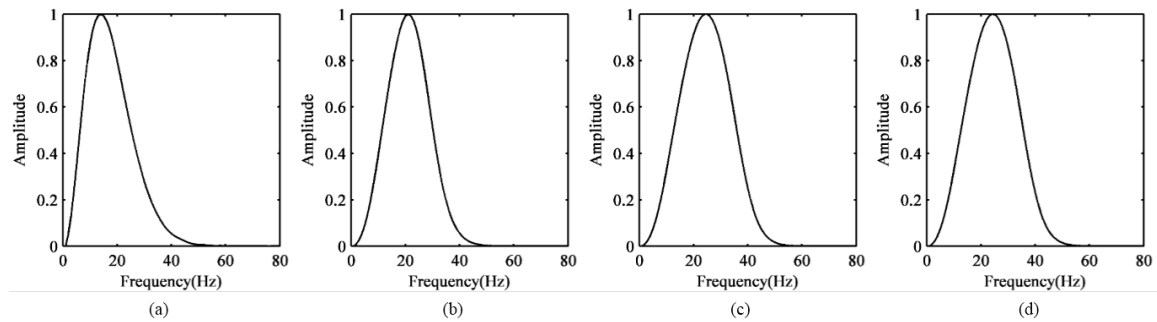


Fig. 4. The amplitude spectrum ($Q = 50$, $t = 1.8$ s) from the red dashed box in Fig. 3. (a) The attenuation amplitude spectrum; (b) The result of the stabilized inverse Q filtering ($L = 20$ dB); (c) The result of the stabilized inverse Q filtering ($L = 60$ dB); (d) The result of the variable gain-limited inverse Q filtering. Note that the attenuation compensation is improved in the variable gain-limited inverse Q filtering result comparing to the stabilized inverse Q filtering.

To further test the robustness of the proposed method, we repeat the same experiment as in Fig. 3, but with 25 dB random noise as shown in Fig. 5a. Fig. 5b shows the result of stabilized inverse Q filtering with gain limit of 60 dB. Although the amplitude attenuation of seismic wave is well compensated, it cannot effectively suppress high-frequency ambient noise, resulting in a serious decrease in the signal-to-noise ratio in the deeper section. In contrast, variable gain-limited inverse Q filtering method not only compensates the seismic wave attenuation, but also successfully suppresses the high-frequency ambient noise, improving the seismic resolution and preserving the signal-to-noise ratio, as shown in Fig. 5c. Therefore, the variable gain-limited inverse Q filtering is a more stable and feasible inverse Q filtering method compared with conventional inverse Q filtering method.

Field data application

In order to compare the effectiveness and stability of the proposed method we apply the variable gain-limited inverse Q filtering method to the field seismic data from Western china, as shown in Fig. 6. Fig. 6a is a seismic amplitude profile from poststack time migration, and figure 6b is the corresponding result from the proposed variable gain-limited inverse Q filtering. Comparing the two figures, the seismic resolution is obviously improved after the inverse Q filtering, with thinner seismic events, enhanced energy, and sharpened stratigraphic and structural discontinuities.

In Fig. 7, we show the advantage using variable gain-limited inverse Q filtering method. Fig. 7a shows a partial enlarged view of the area within the yellow dashed box in Fig. 6a. Figs. 7b and 7c show the results of stabilized

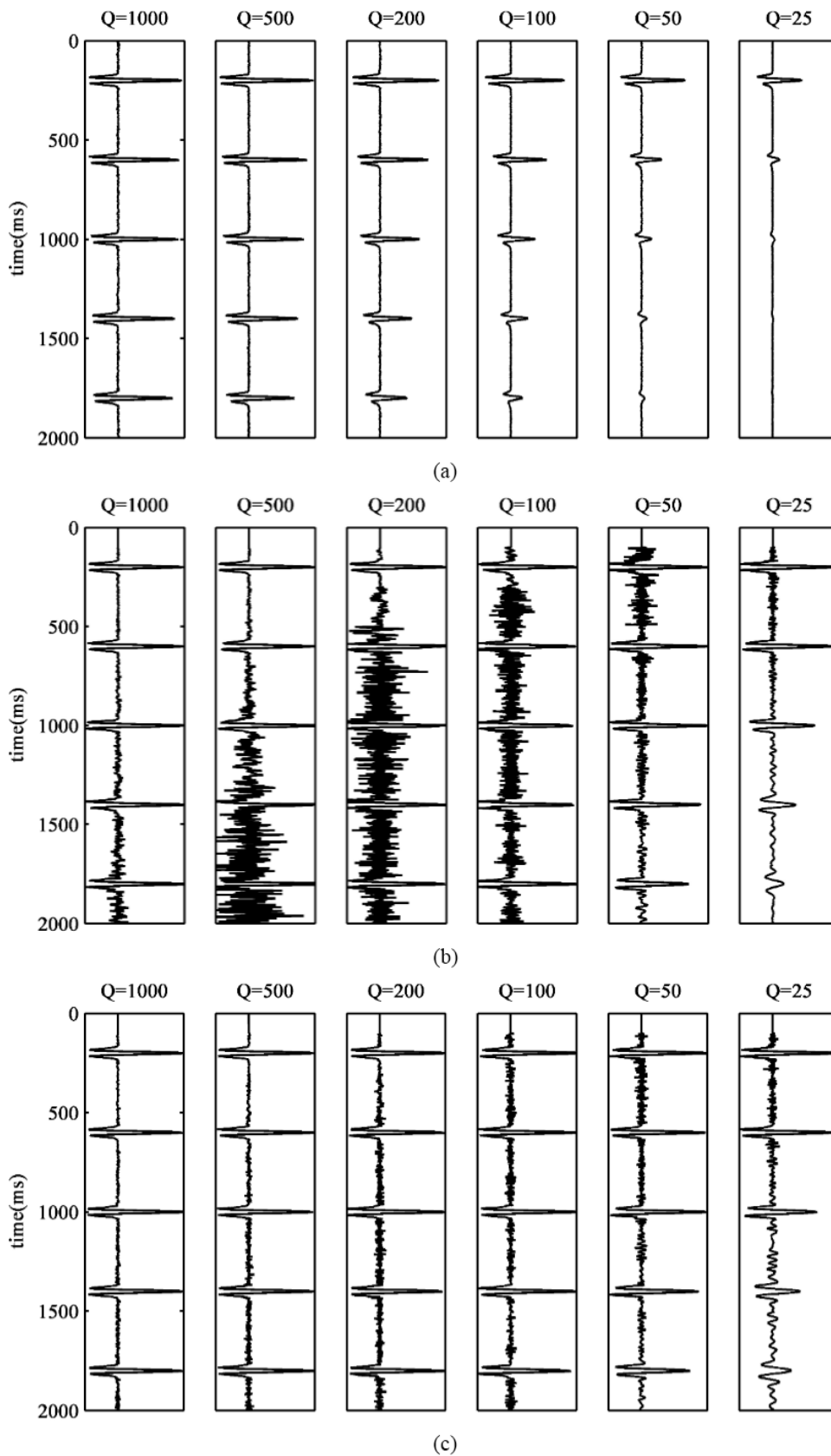


Fig. 5. Synthetic traces with varies degree of random noise and the results from the two inverse Q filtering algorithms. (a) Synthetic seismic traces with weak random noise (signal-to-noise ratio 25 dB); (b) The stabilized inverse Q filtering ($L = 60$ dB) boosts the noise; (c) Variable gain-limited inverse Q filtering produces a result with a much higher signal-to-noise ratio, compared with the stabilized inverse Q filtering ($L = 60$ dB) result.

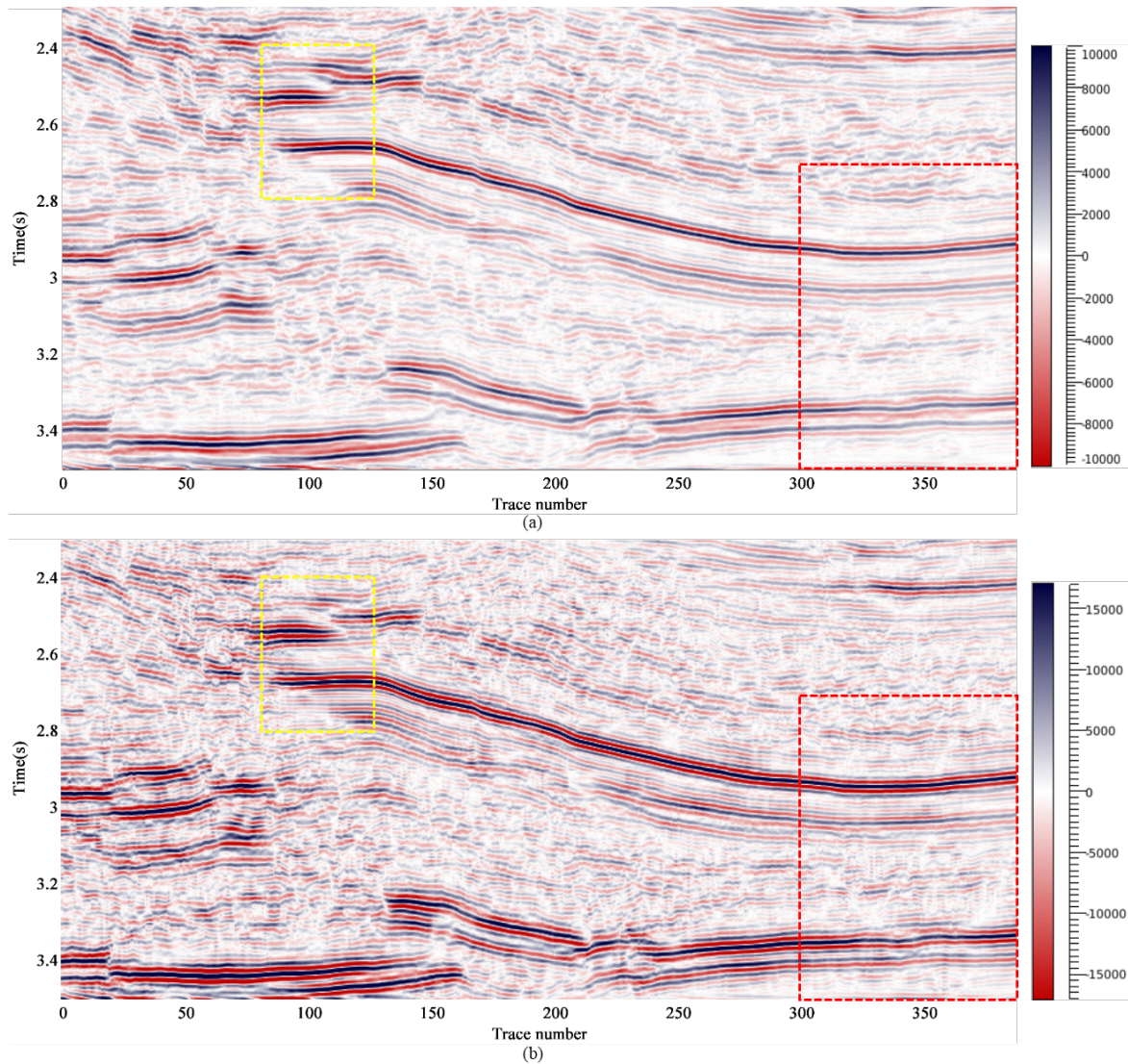


Fig. 6. (a) The poststack time migration profile and (b) the result of variable gain-limited inverse Q filtering. The variable gain-limited scheme improves the interpretability of the seismic section by increasing the frequency bandwidth without degrading the signal-to-noise ratio.

inverse Q filtering with 10 dB and 30 dB gain limit from the same area, respectively. Fig. 7d is the result of the variable gain-limited inverse Q filtering from the same area. Comparing to the results from stabilized inverse Q filtering, we observe that the result from variable gain-limited inverse Q filtering provides more details and crisper image of the fault pointed by black arrows. Fig. 8a shows a partial enlarged view of the area within the red dashed box in Fig. 6a. Fig. 8b and 8c also show the results of the stabilized inverse Q filtering with 10 dB and 30 dB gain limit from the same area, respectively. In Fig. 8d, a partial enlarged view of the red dashed box in Fig. 6b is showed using the proposed method. As shown in Fig. 8b, when the gain limit is 10 dB, the stabilized inverse Q filtering result is less than optimal with decreased resolution. When setting gain limit to 30 dB, the

resolution is effectively improved. Comparing to the results from stabilized inverse Q filtering, in Fig. 8d we observe that more geological structure details are better recovered from the seismic data using the proposed method, such as more continuous reflectors and improved resolution, lightened by black arrows.

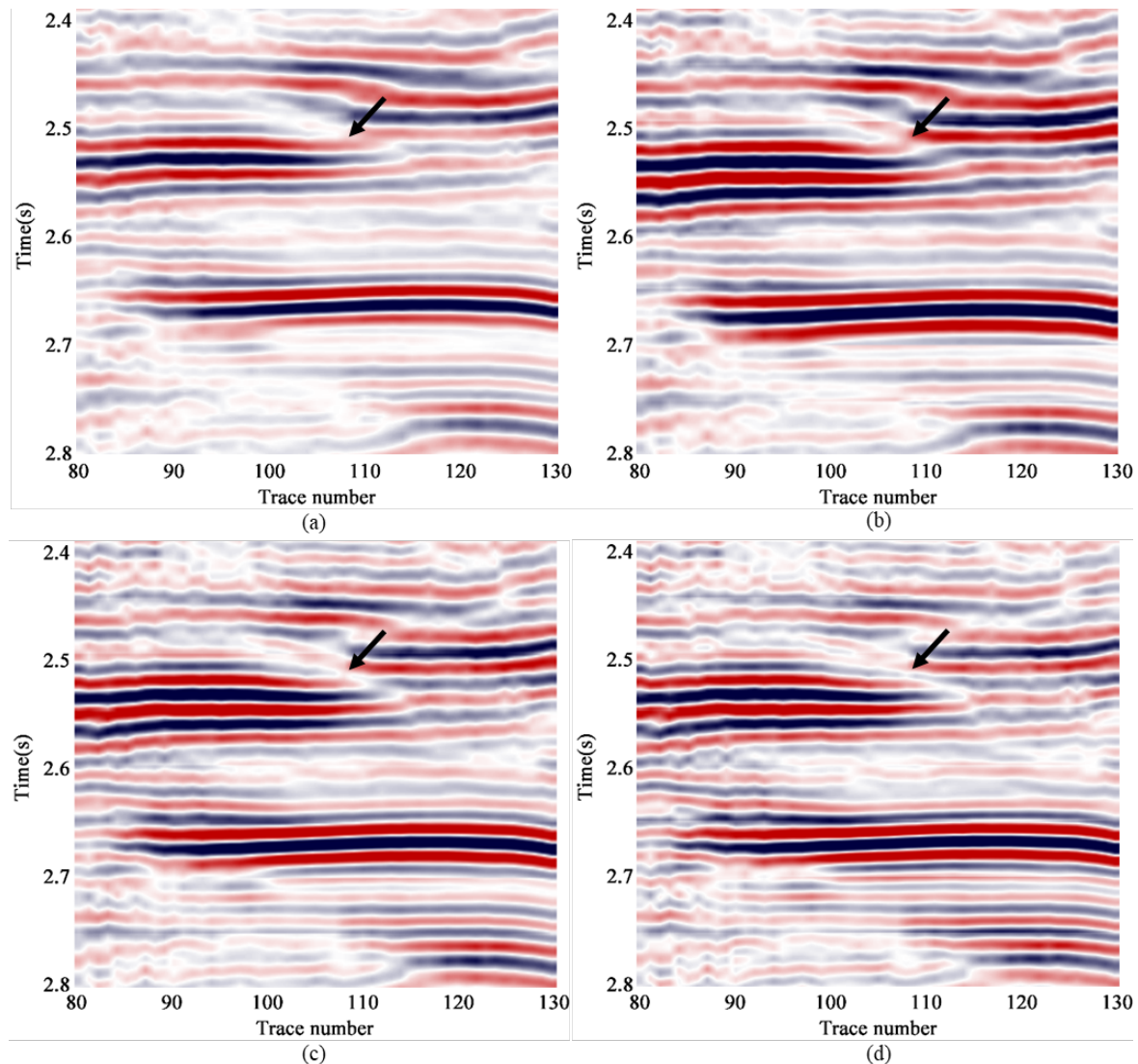


Fig. 7. (a) The partial enlarged view of the yellow dashed box on the left side in Fig. 6a. (b) and (c) are the results of stabilized inverse Q filtering with gain limit set to 10 dB and 30 dB, respectively. (d) The result of variable gain-limited inverse Q filtering. Comparing to the results from stabilized inverse Q filtering, we observe that the result from variable gain-limited inverse Q filtering provides more details and crisper image of the fault.

Fig. 9 shows the normalized smooth average amplitude spectra of the seismic profiles corresponding to Figs. 8a-d. In this figure, the blue curve denotes the average amplitude spectrum before inverse Q filtering (Fig. 6a), the purple and green curves denote the average amplitude spectra after stabilized inverse Q filtering with 10 dB and 30 dB gain limit, respectively,

and the red curve is the average amplitude spectrum after the variable gain-limited inverse Q filtering. Note that after inverse Q filtering, the seismic frequency band becomes broader. Among the three filtered results, the result from the variable gain-limited inverse Q filtering provides the best compensation, which provides the greatest frequency band extension and highest dominant frequency.

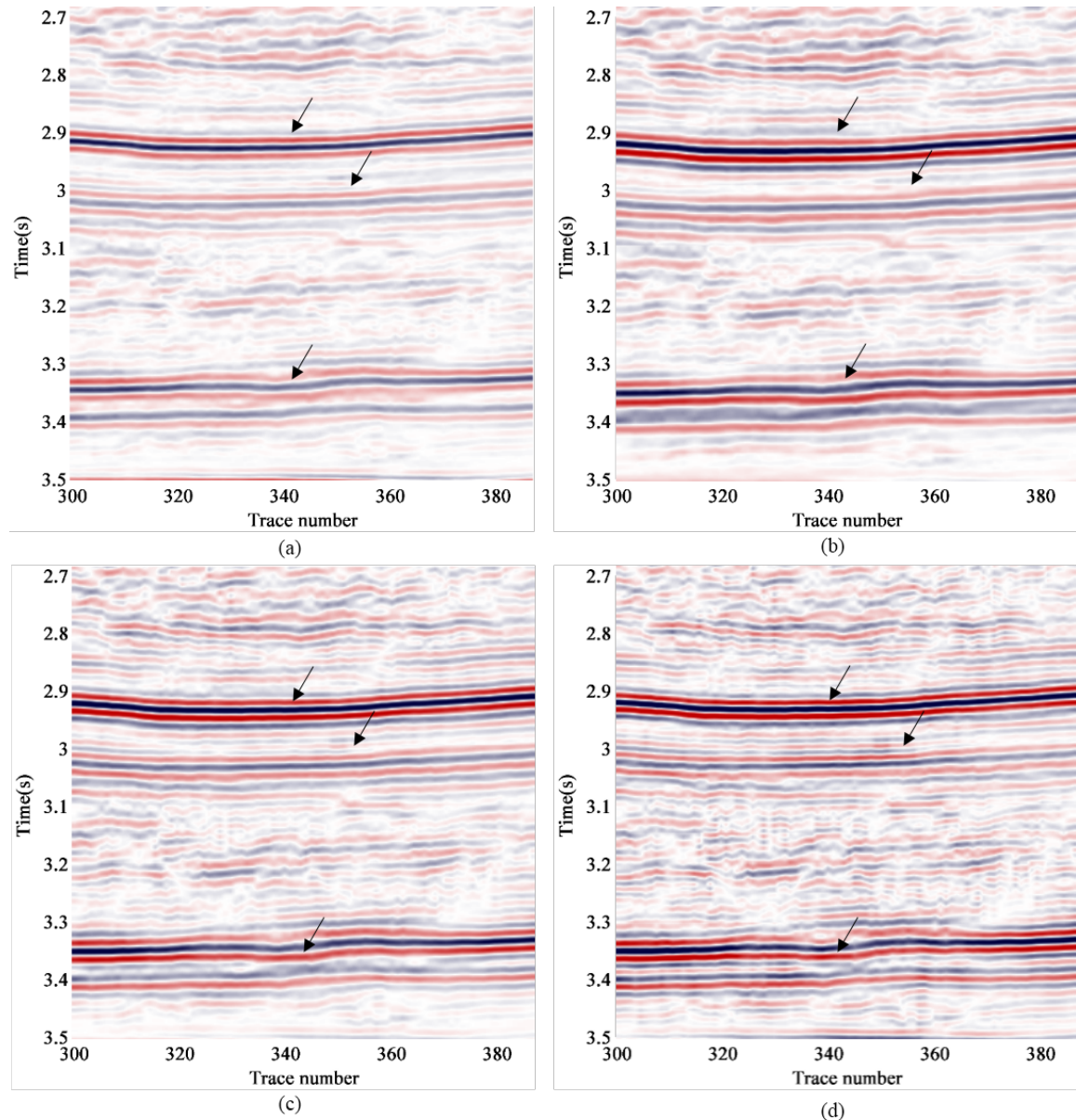


Fig. 8. (a) The partial enlarged view of the red dashed box in the lower right corner of Figs. 6a. (b) and (c) are the results of the stabilized inverse Q filtering with gain limit set to 10 dB and 30 dB, respectively. 10 dB gain limit decreases the seismic resolution. 30 dB gain limit effectively improves the resolution. (d) The partial enlarged view of the red dashed box in the lower right corner in Fig. 6b. Comparing to the results from stabilized inverse Q filtering, we observe that the seismic profile details are more clearly with the proposed methods, details are better recovered from the seismic data, with and the stratigraphic landscape is more continuous reflectors and improved resolution.

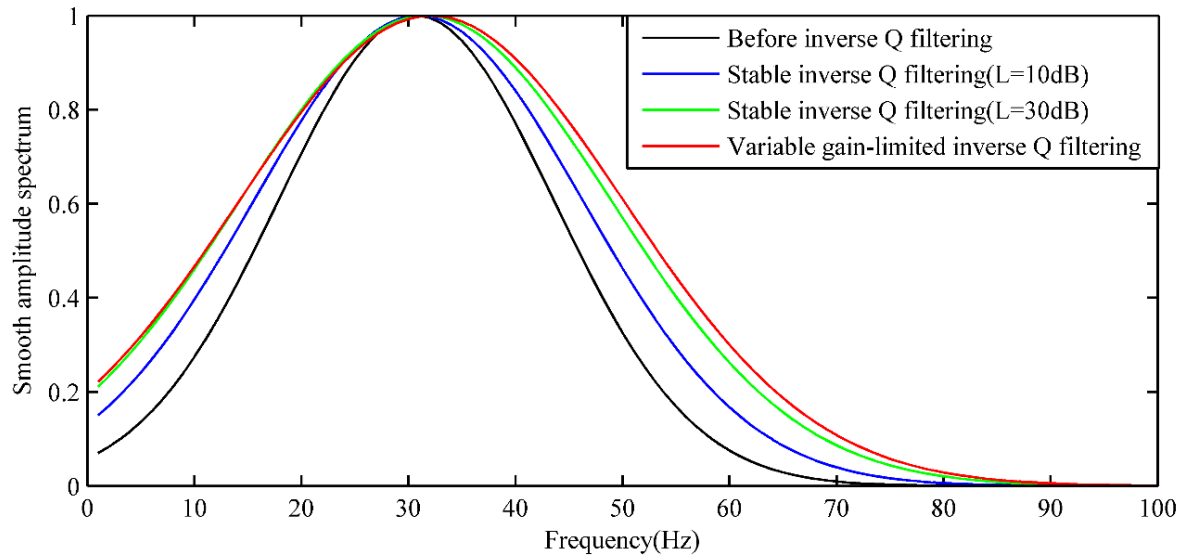


Fig. 9. The average amplitude spectra of the seismic profiles shown in Fig. 8. The amplitude spectra are smoothed and normalized. The blue curve is the original average amplitude spectrum; the purple curve and the green curve are the average amplitude spectra after stabilized inverse Q filtering with gain limit set to 10 dB and 30 dB, respectively; the red curve is the average amplitude spectrum after the variable gain-limited inverse Q filtering. Note that after inverse Q filtering, the seismic frequency band becomes broader. Among the three filtered results, the result from the variable gain-limited inverse Q filtering provides the best compensation, which provides the greatest frequency band extension and highest dominant frequency.

For demonstrating the robustness for field data, next we apply the variable gain-limited inverse Q filtering to the seismic data with poor signal-to-noise ratio, analyzing its capability of noise suppression. Fig. 10a shows a poststack time migrated seismic data with low signal-to-noise ratio. The results from stabilized inverse Q filtering with 10 dB and 50 dB gain limit and variable gain-limited inverse Q filtering are shown in Figs. 10b, 10c, 10d, respectively. The stabilized inverse Q filtering with 10 dB gain limit reduces the resolution, while the 50 dB gain limit results in decreased signal-to-noise ratio. In contrast, in Fig. 10d the variable gain-limited inverse Q filtering provides not only improved resolution, but also preserved signal-to-noise ratio without boosting the noise.

To quantitatively evaluate the results applied by two inverse Q filtering method, Fig. 11 shows the normalized smooth average amplitude spectra from the seismic profiles in Fig. 10. In this figure, the blue curve denotes the average amplitude spectrum before inverse Q filtering, the purple and green curves denote the average amplitude spectra after stabilized inverse Q filtering with 10 dB and 50 dB gain limit, respectively, and the red curve is the average amplitude spectrum after the variable gain-limited inverse Q filtering. Comparing these four amplitude spectra, we conclude that the

stabilized inverse Q filtering with 50 dB gain limit provides the most bandwidth extension at the expense of signal-to-noise ratio. The variable gain-limited inverse Q filtering not only effectively broadens the frequency band, but also suppresses noise much more effectively than the stabilized inverse Q filtering.

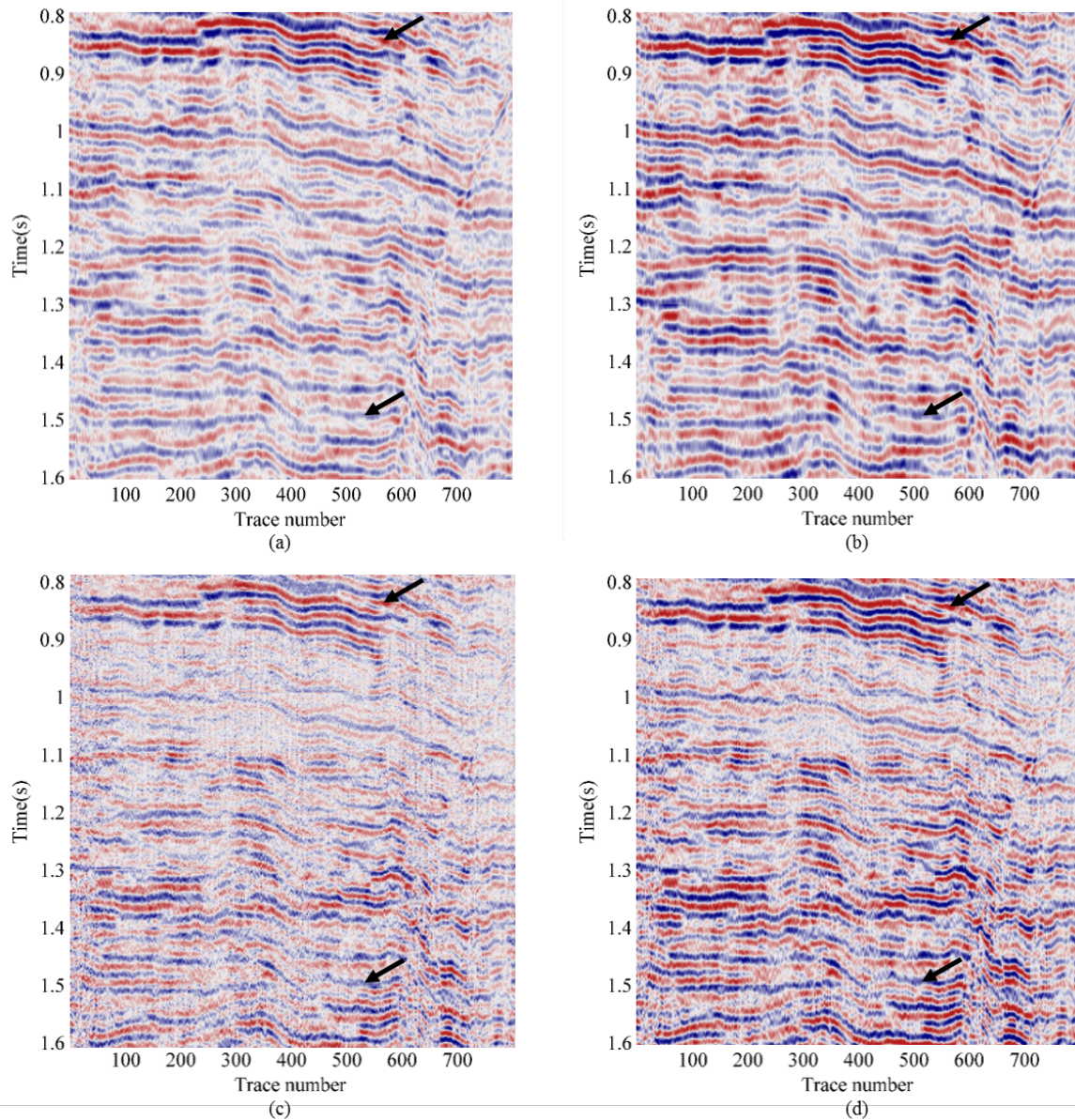


Fig. 10. (a) The poststack time migration profile with low signal-to-noise ratio. (b) and (c) are the results of the stabilized inverse Q filtering with gain limit set to 10 dB and 50 dB, respectively. (d) The result of variable gain-limited inverse Q filtering. The stabilized inverse Q filtering with 10dB gain limit reduces the resolution, while the 50dB gain limited results in decreased signal-to-noise ratio. In contrast, the variable gain-limited inverse Q filtering provides not only improved resolution, but also increased signal-to-noise ratio.

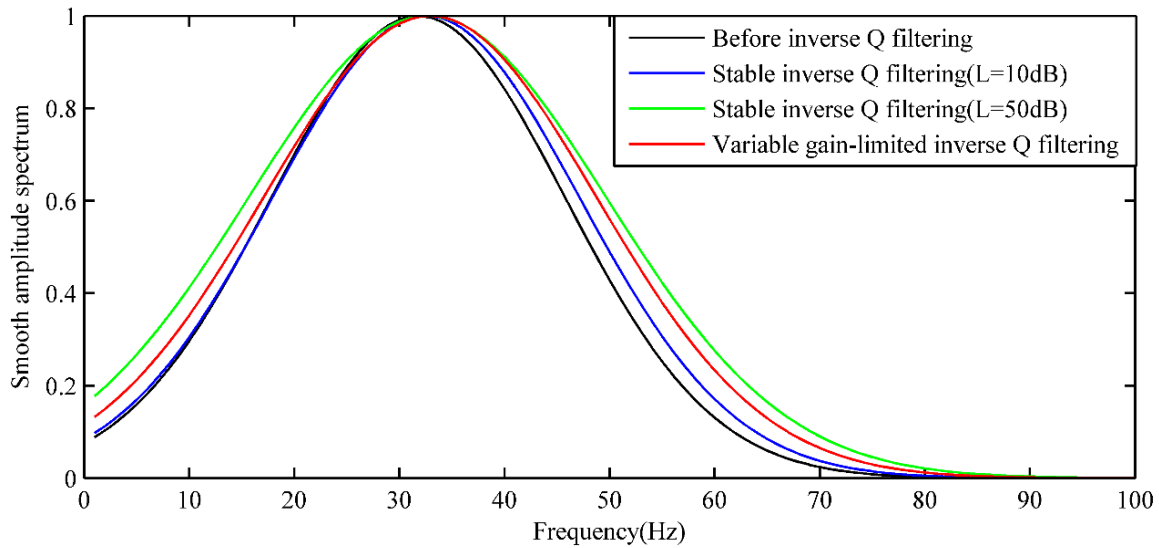


Fig. 11. The average amplitude spectra of the profiles in Fig. 10. The stabilized inverse Q filtering with 50dB gain limit provides the most bandwidth extension at the expense of signal-to-noise ratio. The variable gain-limited inverse Q filtering not only effectively broadens the frequency band, but also suppresses noise much more effectively than the stabilized inverse Q filtering.

Finally, we apply the variable gain-limited inverse Q filtering method to the field seismic data acquired from the South China Sea, as shown in Fig. 12. An effective Q filtering extends the frequency bandwidth and improves the signal-to-noise ratio, therefore improving the quality of subsequent seismic inversion and attribute extraction products. Fig. 12a shows the original poststack time migrated seismic profile, and Fig. 12b shows the result from variable gain-limited inverse Q filtering. Comparing the two images, the proposed inverse Q filtering method greatly enhances seismic resolution and compensates energy attenuation without boosting the noise. Figs. 13a and 13b are partial enlarged view of the black dashed boxes in Figs. 12a and 12b, respectively. We are able to see more details from the filtered result, and the stratigraphic landscape also shows improved continuity after the proposed inverse Q filtering.

To validate the reliability of the processed result using log information, we observe a better correlation between the density log and the profile after inverse Q filtering. Figs. 14a and 14b show the P-impedance inversion results based on field data before and after inverse Q filtering, respectively. A better quality of P-impedance inversion result is acquired based on field data after using inverse Q filtering proposed in this paper. As indicated by the black arrow in the Fig. 14b, one gas-bearing thin layer is identified. We also confirm the gas sand containing calcium interlayer indicated by the blue

arrow. In addition, as indicated by the red arrow in the Fig. 14b, oil-1 and oil-2 layers can be effectively identified and meticulously characterized, which is proved by drilling well. Inversion profiles obtained by using inverse Q filtering data show a better correspondence with calcium content curves and sandstone content curves. Therefore, application for field data shows that the variable gain-limited inverse Q filtering not only can broaden seismic frequency band, improve seismic resolution and also increase the inversion accuracy, which can help to provide foundation of seismic reservoir prediction.

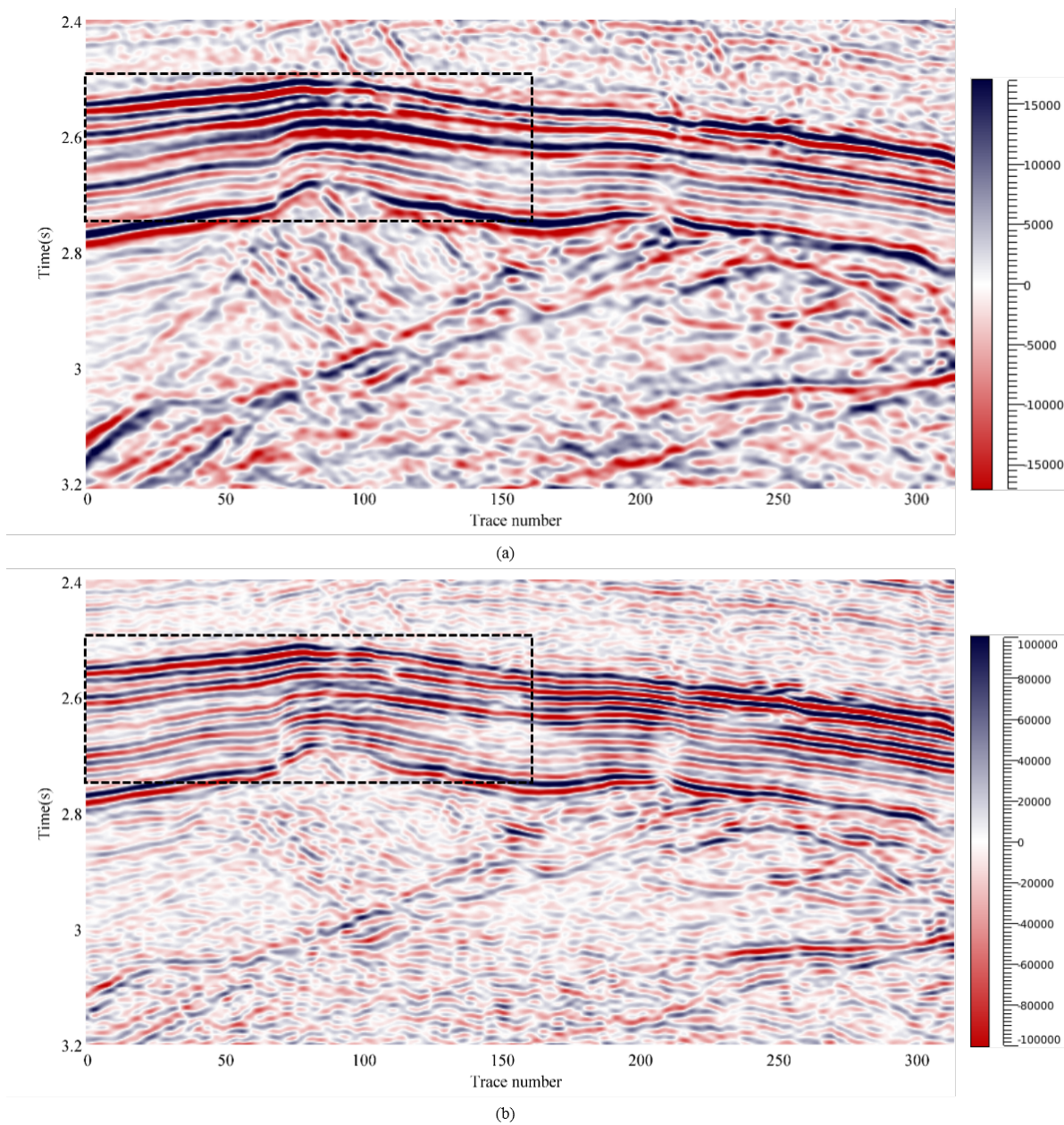


Fig. 12. (a) The post-stack time migration profile from a South China Sea survey, and (b) the result of variable gain-limited inverse Q filtering. Any improvement in continuity of the events in this section should be reliable, because the inverse Q filtering algorithm works purely trace-by-trace.

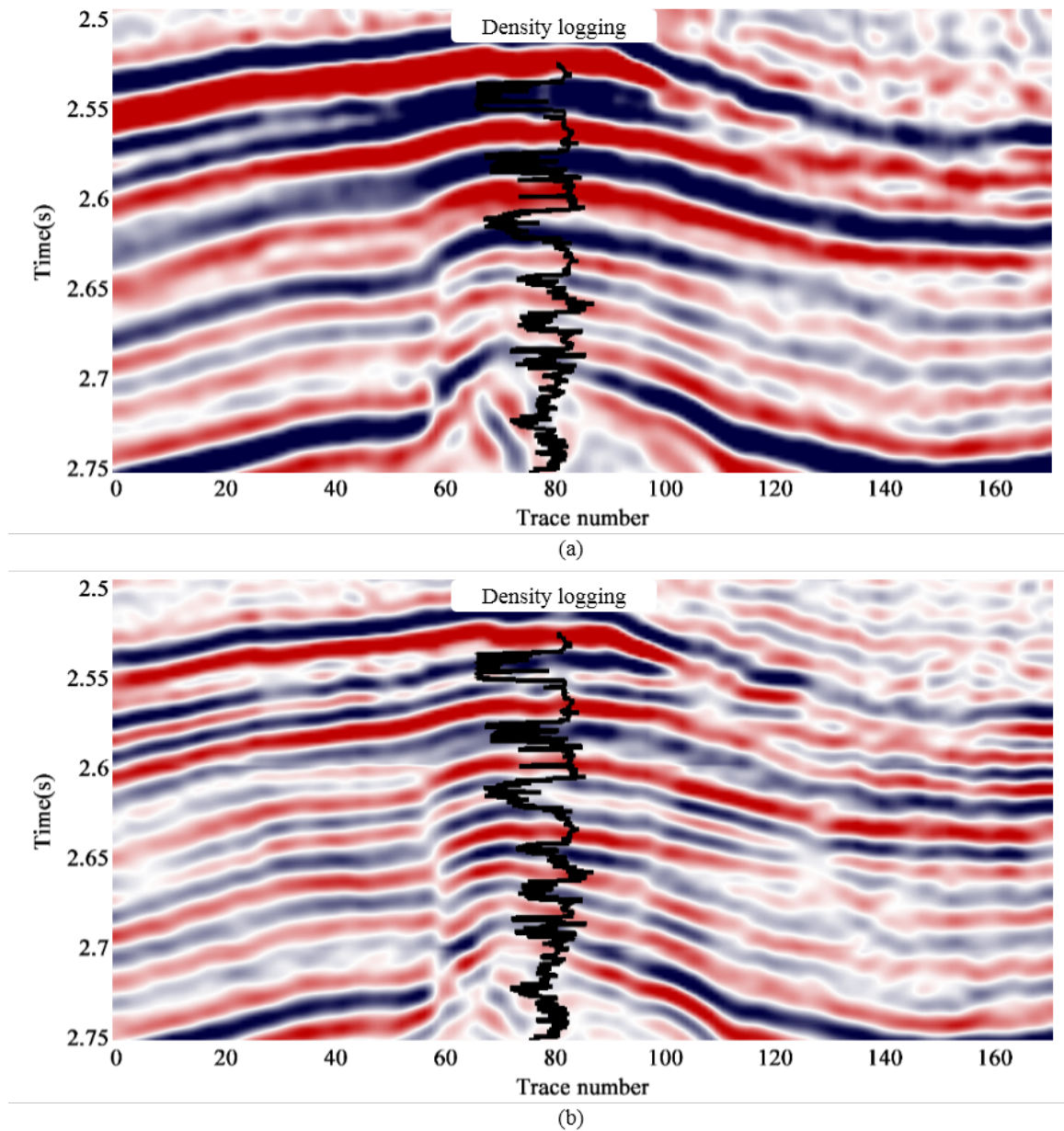


Fig. 13. (a) The partial enlarged view of the black dashed box in Fig. 12a overlaid by density log and (b) the result of variable gain-limited inverse Q filtering from the same region overlaid by density log. We are able to see more details from the filtered result, and the stratigraphic landscape also shows improved continuity after the proposed inverse Q filtering. To validate the result with geologic ground truth, we observe a better correlation between the density log and the profile after inverse Q filtering.

CONCLUSIONS

The stabilized inverse Q filtering method provides the basis for more improved resolution of seismic data. Based on the previous inverse Q algorithms, we developed a variable gain-limited inverse Q filtering method. The proposed method enables gain limit and stabilization factor to vary with time and layer Q , resulting in more stable and effective gain control. Application to synthetic and field data shows that the improved method can

effectively achieve adequate deep section amplitude compensation while suppressing high-frequency environmental noise, which otherwise are difficult with inappropriate stabilization factors. Synthetic test and field application results confirm the improved performance of the proposed method versus the traditional stabilized inverse Q filtering. Furthermore, application to the inversion of then enhanced resolution field data shows that we can effectively improve the inversion accuracy and provide inversion results for the prediction and contribute to detailed description of the reservoir.

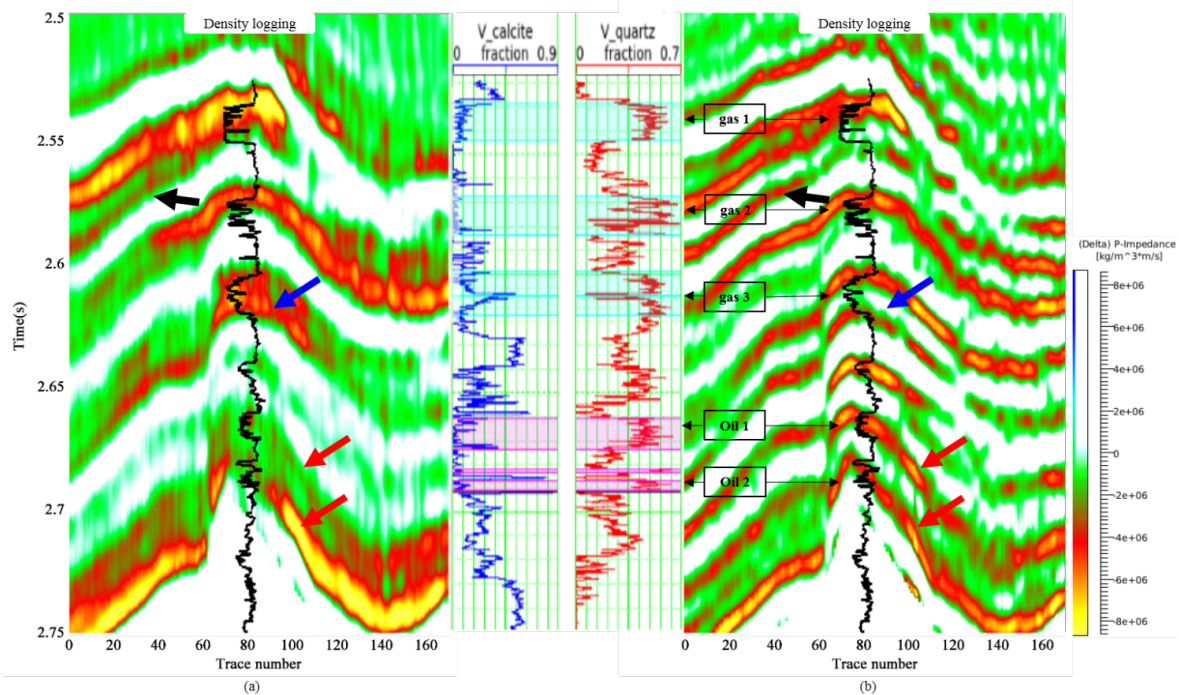


Fig. 14. (a) P-impedance inversion result before inverse Q filtering (Figs. 13a and 13b) P-impedance inversion result after inverse Q filtering (Fig. 13b). A better quality of P-impedance inversion result is acquired based on field data after using inverse Q filtering proposed in this paper. As indicated by the black arrow in the Fig. 14b, one gas-bearing thin layer is identified. We also confirm the gas sand containing calcium interlayer indicated by the blue arrow. In addition, as indicated by the red arrow in the Fig. 14b, oil-1 and oil-2 layers can be effectively identified and meticulously characterized, which is proved by drilling well.

ACKNOWLEDGMENTS

We thank the Key Lab of Earth Exploration and Information Techniques of the Ministry of Education in Chengdu University of Technology for providing the support. The second author (corresponding author) thanks Professor H.D. Chen of Chengdu University of Technology for his beneficial suggestion. This work is financially supported by the national science and technology major project topic of China (Grant No. 2016ZX05026-001-005). We also thank the CNOOC Research Institute for providing the data and support.

REFERENCES

- Bickel, S.H. and Natarajan, R.R., 1985. Plane-wave Q deconvolution, *Geophysics*, 50: 1426-1439.
- Chen, Z.B., Chen, X.H., Li, J.Y., Wang, B.F. and Ma, S., 2014. A band-limited and robust inverse Q filtering algorithm, *Oil Geophys. Prosp.* (in Chinese), 49: 68-75.
- Futterman, W.I., 1962. Dispersive body waves, *J. Geophys. Res.*, 69: 5279-5291.
- Hale, D., 1981. Q and Adaptive Prediction Error Filters. Stanford Exploration Project Rep., 28: 209-231.
- Hale, D., 1982. An inverse Q -filter. Stanford Exploration Project Report., 26: 231-243.
- Hargreaves, N.D. and Calvert, A.J., 1991. Inverse Q filtering by Fourier transform. *Geophysics*, 56: 519-527.
- Hargreaves, N.D., 1992. Similarity and the inverse Q filter: some simple algorithms for inverse Q filtering. *Geophysics*, 57: 944-947.
- Kjartansson, E., 1979. Constant Q wave propagation and attenuation, *J. Geophys. Res.*, 84(B9): 4737-4748.
- Liu, C., Feng, H. and Zhang, J., 2013. Stable iterative method of inverse Q filter. *Petrol. Geophys. Prosp.*, 48: 890-895.
- Margrave, G.F., Lamoureux, M.P. and Grossman, J.P., 2002. Gabor deconvolution of seismic data for source waveform and Q correction. Expanded Abstr., 72nd Ann. Internat. SEG Mtg., Salt Lake City: 2190-2193.
- Margrave, G.F., Lamoureux, M.P. and Henley, D.C., 2011. Gabor deconvolution: Estimating reflectivity by nonstationary deconvolution of seismic data. *Geophysics*, 76(3): W15-W30.
- Stolt, R., 1978. Migration by Fourier transform, *Geophysics*, 43: 23-48.
- Wang, Y.H., 2002. A stable and efficient approach of inverse Q filtering, *Geophysics*, 67: 657-663.
- Wang, Y.H., 2003. Quantifying the effectiveness of stabilized inverse Q -filtering. *Geophysics*, 68: 337-345.
- Wang, Y.H., 2004. Modified Kolsky model for seismic attenuation and dispersion. *J. Geophys. Engineer.*, 1(3): 187-196.
- Wang, Y.H., 2006. Inverse Q -filter for seismic resolution enhancement, *Geophysics*, 71: 351-360.
- Wang, Y.H., 2008. *Seismic Inverse Q Filtering*. Blackwell Scientific Publishing, Oxford.
- Wang, Y.H., 2014. Stable Q analysis on vertical seismic profiling data. *Geophysics*, 79(4), D217-D225.
- Wu, J.Z., Yang, X.L. and Long, Y., 2016. A robust approach of inverse Q filtering with equivalent Q . *Petrol. Geophys. Prosp.*, 51: 63-70.
- Yao, Z.X., Gao, X. and Li, W.X., 2003. The forward Q method for compensating attenuation and frequency dispersion used in the seismic profile of depth domain. *J. Geophys.*, 46: 229-230.
- Yan, H.Y., Liu, Y. and Zhao, Q.H., 2011. A method for improving VSP resolution by inverse Q filtering. *OGP*, 46: 873-880.
- Zhou, H.L., Tian, Y.M. and Ye, Y., 2014. Dynamic deconvolution of seismic data based on generalized S-transform. *J. Appl. Geophys.*, 10(8): 1-11.
- Zhou, H.L., Wang, C.C., Marfurt, K.J., Jian, Y.W. and Bi, J.X., 2016. Enhancing the resolution of non-stationary seismic data using improved time-frequency spectral modelling. *Geophys. J. Internat.*, 20(5): 203-219.
- Zhang, G.L., He, Z.H. and Wang, X.M., 2015. A self-adaptive approach for inverse Q -filtering, *Chin. J. Geophys.* (in Chinese), 57: 1655-1663.
doi: 10.6038/cjg20140528.